Inorg. Chem. **2006**, *45*, 2242−2250

Synthesis of Zinc, Copper, Nickel, Cobalt, and Iron Complexes Using Tris(pyrazolyl)methane Sulfonate Ligands: A Structural Model for N,N,O Binding in Metalloenzymes

Elizabeth T. Papish,*,† Michael T. Taylor,† Finith E. Jernigan III,† Michael J. Rodig,† Robert R. Shawhan,† Glenn P. A. Yap,‡ and Fernando A. Jové‡

Departments of Chemistry, Salisbury University, 1101 Camden Avenue, Salisbury, Maryland 21801, and University of Delaware, Newark, Delaware 19716

Received September 14, 2005

Ligands of intermediate steric bulk were designed to mimic metalloenzymes with histidine and carboxlyate binding sites. The reaction between tris(3-isopropylpyrazolyl)methane and butyllithium followed by SO_3NMe_3 in THF yielded the new ligand lithium tris(3-isopropylpyrazolyl)methane sulfonate ($LiTpms^{iPr}$). Various metal salts reacted with $LiTpms^{iPr}$ to give the octahedral complexes $M(Tpms^{iPr})_2$ (M = Zn, Cu, Ni, Co, Fe) in which each ligand has N,N,O binding to the metal. In the reaction between $LiTpms^{iPr}$ and $ZnCl_2$, in addition to the major product $Zn(Tpms^{iPr})_2$, $[LiTpms^{iPr}\text{-}ZnCl_2]\cdot 2THF$ was also formed as a minor product with a tetrahedral zinc atom coordinated to either N,N,Cl,Cl in the solid phase or N,N,N,Cl in acetonitrile solution. Although $Tpms^{iPr}$ is coordinatively flexible and can act as a bipodal or tripodal ligand, it appears to favor the formation of octahedral L_2M complexes.

Introduction

Our aim is to provide an improved structural model for biologically important metalloenzymes that utilize a 2-His-1-carboxylate motif. These enzymes use a wide variety of metals, but the most common biologically active metals are the late first row transition metals (e.g., Zn^{2+} in phosphotriesterase (PTE),[1] thermolysin and carboxypeptidase A;[2] Ni^{2+} in urease;[3] and Fe^{2+} in tyrosine hydroxylase, dioxygenases, and isopenicillin N synthase).[4] Additionally, many of these enzymes exhibit comparable activity upon substitution with Cu^{2+} or Co^{2+}, and the improved spectroscopic properties of these metals make them important structural and functional probes.[2,5] The diverse chemical functions of structurally similar enzymes warrant a systematic investigation of how changing the identity of the metal changes the structure of model compounds.

Tris(pyrazolyl)borate (Tp) complexes with N,N,N ligation have been used to model several 2-His-1-carboxylate enzymes, despite the drawbacks in terms of the lack of an O donor, because they are relatively easy to synthesize and modify.[6,7,8,9] The first step in devising a better 2-His-1-carboxylate enzyme mimic would seem to be replacing the N,N,N ligation in Tp complexes with N,N,O. Although there has recently been an increase in contributions to the field of N,N,O facially coordinating ligands,[10] the systematic effects

* To whom correspondence should be addressed. E-mail: etpapish@salisbury.edu.

† Salisbury University.

‡ University of Delaware.

(1) Omburo, G. A.; Kuo, J. M.; Mullins, L. S.; Raushel, F. M. *J. Biol. Chem.* **1992**, *267*, 13278−13283. (b) diSoudi, B.; Grimsley, J. K.; Lai, K.; Wild, J. R. *Biochemistry* **1999**, *38*, 2866−2872. (c) Dumas, D. P.; Durst, H. D.; Landis, W. G.; Raushel, F. M.; Wild, J. R. *Arch. Biochem. Biophys.* **1990**, *277*, 155−159. (d) Benning, M. W.; Shim, H.; Raushel, F. M.; Holden, H. M. *Biochemistry* **2001**, *40*, 2712−2722.

(2) Parkin, G. *Chem. Rev.* **2004**, *104*, 699−767.

(3) Sumner, J. B. *J. Biol. Chem.* **1926**, *69*, 435−441. (b) Dixon, N. E.; Gazzola, C.; Blakeley, R. L.; Zerner, B. *J. Am. Chem. Soc.* **1975**, *97*, 4131−4132. (c) Pearson, M. A.; Michel, L. O.; Hausinger, R. P.; Karplus, P. A. *Biochemistry* **1997**, *36*, 8164−8172. (d) Benini, S.; Rypniewski, W. R.; Wilson, K. S.; Miletti, S.; Ciurli, S.; Mangani, S. *J. Biol. Inorg. Chem.* **20000**, *5*, 110−118. (e) Blakeley, R. L.; Treston, A.; Andrews, R. K.; Zerner, B. *J. Am. Chem. Soc.* **1982**, *104*, 612−614.

(4) Koehntop, K. D.; Emerson, J. P.; Que, L. Jr. *J. Biol. Inorg. Chem.* **2005**, *10*, 87−93.

(5) Bertini, I.; Luchinat, C. *Bioinorganic Chemistry;* Bertini, I., Gray, H. B., Lippard, S. J., Valentine, S. J., Eds.; University Science Books: Mill Valley, CA, 1994; pp 37−106.

(6) Trofimenko, S. *J. Am. Chem. Soc.* **1966**, *88*, 1842−1844. (b) Trofimenko, S. *Chem. Rev.* **1993**, *93*, 943−980. (c) Trofimenko, S. *Scorpionates: The Coordination Chemistry of Polypyrazolylborate Ligands*; Imperial College Press: London, 1999. (d) Looney, A.; Han, R.; McNeill, K.; Parkin, G. *J. Am. Chem. Soc.* **1993**, *115*, 4690−4697. (e) Parkin, G. *Chem. Commun.* **2000**, 1971−1985. (f) Vahrenkamp, H. *Acc. Chem. Res.* **1999**, *32*, 589−596.

(7) Trofimenko, S. *J. Am. Chem. Soc.* **1967**, *89*, 3170. (b) Trofimenko, S. *J. Am. Chem. Soc.* **1967**, *89*, 6288.

10.1021/ic051579a CCC: $33.50
Published on Web 01/31/2006

Scheme 1

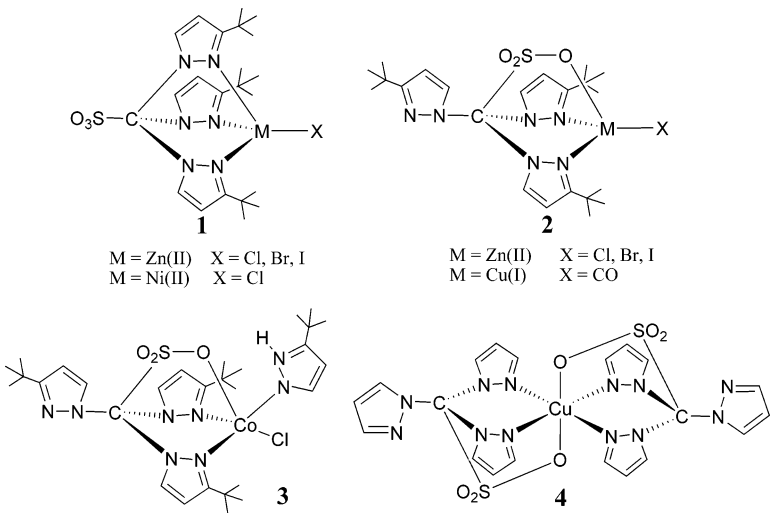

of steric tuning with ligands of intermediate bulk are thus far insufficient to find patterns of reactivity.

Octahedral L_2M sandwich complexes with an N_4O_2 donor set are found with a wide variety of N,N,O ligands.[11,12] Typically, model compounds have included pyrazole rings as N donors and carboxylates[13] or phenolates[14,15,16] as O donors. We were interested in the tris(pyrazolyl)methane sulfonate ligand (Tpms) because it was reported to be water-soluble and coordinatively flexible.[17] The Tpms ligand was first synthesized by Kläui et al. as Tpms and Tpms^{tBu}. Tpms^{tBu} has been shown to bind through either N,N,N or N,N,O in zinc, nickel, and cobalt complexes with coordination numbers four (**1** and **2**) and five (**3**) (Scheme 1).[17c] In contrast Tpms exhibits N,N,O binding to Cu^{2+} with coordination number six (**4**), as characterized by IR and elemental analysis.[18]

We were interested in synthesizing model complexes with the tris(3-isopropylpyrazolyl)methane sulfonate (Tpms^{iPr}) ligand (Scheme 2) because of its water-solubility and

Scheme 2

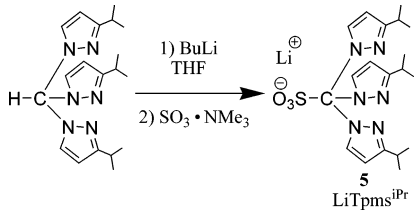

intermediate steric bulk. Our basic questions were as follows. (1) If given a choice between N,N,O versus N,N,N coordination which will the metal prefer? (2) Will a ligand of intermediate steric bulk favor the formation of four-, five-, or six-coordinate complexes? (3) Will the answers to the first two questions vary from one metal to another with the same

(8) Kitajima, N.; Hikichi, S.; Tanaka, M.; Moro-oka, Y. *J. Am. Chem. Soc.* **1993**, *115*, 5496−5508. (b) Kitajima, N.; Osawa, M.; Imai, S.; Fujisawa, K.; Moro-oka, Y.; Heerwegh, K.; Reed, C. A.; Boyd, P. D. W. *Inorg. Chem.* **1994**, *33*, 4613. (c) Kitajima, N.; Tamura, N.; Tanaka, M.; Moro-oka, Y. *Inorg. Chem.* **1992**, *31*, 3342. (d) Kitajima, N.; Tolman, W. B. *Prog. Inorg. Chem.* **1995**, *43*, 419. (e) Kitajima, N.; Fujisawa, K.; Fujimoto, C,; Moro-oka, Y.; Hashimoto, S.; Kitagawa, T.; Toriumi, K.; Tatsumi, K.; Nakamura, A. *J. Am. Chem. Soc.* **1992**, *114*, 1277. (f) Hikichi, S.; Tanaka, M.; Moro-oka, Y.; Kitajima, N. *J. Chem. Soc., Chem. Commun.* **1994**, 1737. (g) Kitajima, N.; Moro-oka, Y. *Chem. Rev.* **1994**, *94*, 737.

(9) Calabrese, J. C.; Trofimenko, S.; Thompson, J. S. *J. Chem. Soc., Chem. Commun.* **1986**, 1122. *(*b) Trofimenko, S.; Calabrese, J. C.; Thompson, J. S. *Inorg. Chem.* **1987**, *26*, 1507.

(10) For a review, see: (a) Otero, A.; Fernández-Baeza, J.; Antiñolo, A.; Tejeda, J.; Lara-Sánchez, A. *Dalton Trans.* **2004**, 1499−1510. Also, see: (b) Dowling, C.; Murphy, V. J.; Parkin, G. *Inorg. Chem.* **1996**, *35*, 2415−2420. (c) Dowling, C.; Parkin, G. *Polyhedron* **1996**, *15*, 2463−2465. (d) Ghosh, P.; Parkin, G. *J. Chem. Soc., Chem. Commun.* **1998**, 413−414. (e) Ghosh, P.; Parkin, G. *J. Chem. Soc., Dalton Trans.* **1998**, 2281−2284. (f) Ortiz, M.; Diaz, A.; Cao, R.; Otero, A.; Fernandez-Baeza, J. *Inorg. Chim. Acta* **2004**, *357*, 19−24. (g) Ortiz, M.; Diaz, A.; Cao, R.; Suardiaz, R.; Otero, A.; Antiñolo, A.; Fernandez-Baeza, J. *Eur. J. Inorg. Chem.* **2004**, 3353−3357.

(11) Many examples of N_4O_2 coordination caused by more than two ligands bound to zinc, nickel, or copper (II), including bis- and tris(pyrazolyl)-borates combined with exogenous O ligands, exist. See: (a) Kisała, J.; Ciunik, Z.; Drabent, K.; Ruman, T.; Wołowiec, S. *Polyhedron* **2003**, *22*, 1645−1652. (b) Rheingold, A. L.; Incarvito, C. D.; Trofimenko, S. *Inorg. Chem.* **2000**, *39*, 5569−5571. (c) Naumov, P.; Jovanovski, G.; Drew, M. G. B.; Ng, S. W. *Inorg. Chim. Acta* **2001**, *314*, 154−162.

(12) Bruijnincx, P. C. A.; Lutz, M.; Spek, A. L.; van Faassen, E. E.; Weckhuysen, B. M.; van Koten, G.; Klein Gebbink, R. J. M. *Eur. J. Inorg. Chem.* **2005**, 779−787.

(13) Beck, A.; Weibert, B.; Burzlaff, N. *Eur. J. Inorg. Chem.* **2001**, 521−527. (b) Beck, A.; Barth, A.; Hübner, E.; Burzlaff, N. *Inorg. Chem.* **2003**, *42*, 7182−7188. (c) Hegelmann, I.; Beck, A.; Eichhorn, C.; Weibert, B.; Burzlaff, N. *Eur. J. Inorg. Chem.* **2003**, 339−347. (d) Burzlaff, N.; Hegelmann, I.; Weibert, B. *J. Organomet. Chem.* **2001**, *626*, 16−23. (e) Hammes, B. S.; Kieber-Emmons, M. T.; Letizia, J. A.; Shirin, Z.; Carrano, C. J.; Zakharov, L. N.; Rheingold, A. L. *Inorg. Chim. Acta* **2003**, *346*, 227−238.

(14) Higgs, T. C.; Carrano, C. J. *Inorg. Chem.* **1997**, *36*, 291. (b) Higgs, T. C.; Carrano, C. J. *Inorg. Chem.* **1997**, *36*, 298. (c) Hammes, B. S.; Carrano, C. J. *Inorg. Chem.* **1999**, *38*, 3562.

(15) For Cu^{2+}, a six coordinate complex was spectroscopically characterized with H and Me pyrazole substituents. Other ligands with H, Me, and *t*Bu pyrazole substituents gave crystallographically characterized five coordinate complexes, see: (a) Higgs, T. C.; Ji, D.; Czernuscewicz, R. S.; Carrano, C. J. *Inorg. Chim. Acta* **1998**, *273*, 14. (b) Warthen, C. R.; Carrano, C. J. *J. Inorg. Biochem.* **2003**, *94*, 197.

(16) Hammes, B. S.; Carrano, C. J. *Inorg. Chem.* **1999**, *38*, 4593.

(17) Kläui, W.; Berghahn, M.; Rheinwald, G.; Lang, H. *Angew. Chem., Int. Ed.* **2000**, *39*, 2464−2466. (b) Kläui, W.; Schramm, D.; Peters, W.; Rheinwald, G.; Lang, H. *Eur. J. Inorg. Chem.* **2001**, 1415−1424. (c) Kläui, W.; Berghahn, M.; Frank, W.; Rei*β*, G. J.; Schönherr, T.; Rheinwald, G.; Lang, H. *Eur. J. Inorg. Chem.* **2003**, 2059−2070.

(18) Santini, C.; Pellei, M.; Lobbia, G. G.; Cingolani, A.; Spagna, R.; Camalli, M. *Inorg. Chem. Commun.* **2002**, *5*, 430−433.

ligand? The rich and varied Tp chemistry shows us that the answers are usually not predictable, and indeed the seemingly minor change from *tert*-butyl to isopropyl at the three position of the pyrazole rings results in dramatically different coordination chemistry and solubility properties.

Experimental

General. All moisture and air-sensitive compounds were stored and measured inside of a glovebox or under N_2 using a Schlenk line. NMR spectra were recorded using a Bruker 400 MHz NMR spectrometer. Infrared (IR) spectra were recorded on a Thermo-Nicolet Avatar 360 FT-IR. UV−vis spectra were recorded on a Beckman Coulter DU 7400 spectrophotometer in CH_2Cl_2 solutions in quartz cuvettes. Elemental analyses were performed by Desert Analytics, Tuscon, AZ. Tris(3-isopropylpyrazolyl) methane, was synthesized using modified literature procedures.[19]

Synthesis of LiTpms^{iPr} (5). Nine milliliters of 2.5 M *n*-butyllithium (0.023 mol) in hexanes was added slowly to 6.134 g (0.01803 mol) Tpm^{iPr} in 30 mL dry THF at −65 °C, and during the addition the temperature did not exceed −45 °C. SO_3NMe_3 (3.037 g, 0.02182 mol) was added, and the reaction was allowed to warm to room temperature overnight. The hexane/THF solvent was removed, yielding a tan solid. The solid was dissolved in 75 mL of warm toluene, and the solution was placed in the freezer. Compound **5** precipitated as a white solid, which was filtered and washed with pentane. Some of the solvent from the filtrate was removed, and pentane was added to precipitate a second batch of **5**. A combined yield of 4.694 g (0.01101 mol) of **5** was obtained. Yield: 61%. ^{1}H NMR ($CDCl_3$): δ 7.20 (br, 3H, 5-pz), 6.15 (br, 3H, 4-pz), 2.88 (m, 3H, Me_2CH), 1.12 (d, 18H, Me_2CH). ^{13}C NMR: δ 162.9 (3-pz), 133.7 (5-pz), 103.6 (4-pz), 94.5 (C−SO_3), 27.5 (Me_2CH), 22.9 (Me_2CH). IR (KBr): ν 3152 (w, ν(C−H)), 2965 (vs, ν(C−H)), 1537 (m, ν(C═C)), 1051 (vs, ν(S−O)), 651 (vs, ν-(C−S)). A satisfactory elemental analysis was not obtained.

Synthesis of Zn(Tpms^{iPr})$_2$ ($\mathbf{6_{Zn}}$). Compound **5** (0.249 g, 0.584 mmol) was mixed with 0.143 g (0.651 mmol) of $Zn(OAc)_2 \cdot 2H_2O$ in 15 mL of CH_2Cl_2. The reaction was stirred overnight, and the solution was then filtered. The solvent was removed from the filtrate, and the solid was dried under vacuum to give 0.196 g (0.217 mmol) of $\mathbf{6}_{Zn}$ in a 74.3% yield. White crystals of $\mathbf{6}_{Zn}$ for single-crystal X-ray diffraction were grown by slow evaporation of a THF/cyclohexane solution. ^{1}H NMR ($CDCl_3$): δ 8.97 (d, 1H, 5-pz), 6.86 (d, 2H, 5-pz), 6.41 (d, 1H, 4-pz), 6.19 (d, 2H, 4-pz), 3.08 (m, 1H, Me_2CH), 2.60 (m, 2H, Me_2CH), 1.31 (d, 6H, Me_2CH), 1.14 (d, 6H, Me_2CH), 1.10 (d, 6H, Me_2CH). ^{13}C NMR: δ 164.5 (3-pz Zn bound), 163.5 (3-pz), 137.1 (5-pz), 134.6 (5-pz Zn bound), 105.3 (4-pz), 103.0 (4-pz Zn bound), 93.9 (C−SO_3), 28.3 (Me_2CH), 26.8 (Me_2CH Zn bound), 26.6 (Me_2CH), 22.8 and 21.1 (Me_2CH Zn bound). NMR assignments have been confirmed by HMQC. IR (KBr): ν 3165, 3124 (w, ν(C−H)), 2971 (vs, ν(C−H)), 1541 (m, ν(C═C)), 1048 (vs, ν(S−O)), 651 (vs, ν(C−S)). Anal. Calcd: 50.44 C, 6.02 H, 18.59 N. Found: 50.49 C, 6.22 H, 18.48 N.

Synthesis of NaTpms^{iPr} (7) from $\mathbf{6_{Zn}}$. Compound $\mathbf{6}_{Zn}$ (0.427 g, 0.472 mmol) and solid NaOH (0.250 g, 6.25 mmol) were dissolved in 40 mL of a 1:1 CH_2Cl_2/H_2O solution. This solution was stirred under a N_2 atmosphere for 72 h, and the solvent was then removed. Acetonitrile was added to the resulting solid; the solution was filtered, and the solvent was removed. Crystals were grown by diffusion of hexane into a THF solution of the product. Yield: 0.305 g (0.689 mmol) (72.9%). NaTpms^{iPr} has solubility properties similar to those of LiTpms^{iPr}, and it is not air sensitive. ^{1}H NMR ($CDCl_3$): δ 7.15 (d, 3H, 5-pz), 6.16 (d, 3H, 4-pz), 2.89 (m, 3H, Me_2CH), 1.10 (d, 18H, Me_2CH). ^{13}C NMR: δ 162.3 (3-pz), 133.6 (5-pz), 103.5 (4-pz), 95.7 (C−SO_3), 27.7 (Me_2CH), 22.9 (Me_2CH). IR (KBr): ν 3149 (w, ν(C−H)), 2966 (vs, ν(C−H)), 1537 (m, ν(C═C)), 1057 (vs, ν(S−O)), 643 (vs, ν(C−S)).

Synthesis of [LiTpms^{iPr}ZnCl$_2$]·2THF (8·2THF) and Characterization in the Solid Phase. $ZnCl_2$ (0.400 g, 2.94 mmol) was added to 0.998 g (2.34 mmol) of **5** in 30 mL of methanol, and the mixture was stirred for 6 h. The solvent was removed, and the resulting solid was dissolved in a minimal amount of CH_2Cl_2 and filtered to remove unreacted $ZnCl_2$. Hexane was slowly added to the filtrate until a white solid precipitated, and a second filtration was performed to yield 0.365 g of a mixture of two products, one of which is Zn(Tpms^{iPr})$_2$ by ^{1}H and ^{13}C NMR and IR spectroscopy. The white solid was recrystallized twice, each time by dissolving it in THF and slowly adding cyclohexane. Single-crystal X-ray diffraction indicated that the crystals formed were **8**·2THF, obtained in a 6.0% yield (99 mg, 0.14 mmol). IR (KBr): ν 3162, 3124 (w, ν(C−H)), 2970 (vs, ν(C−H)), 1542 (m, ν(C═C)), 1048 (vs, ν(S−O)), 639 (vs, ν(C−S)). A satisfactory elemental analysis was not obtained.

Characterization of 8·2THF in Solution. The crystals of **8**·2THF had low solubility in $CDCl_3$, but small peaks were detectable in the ^{1}H NMR; the same peaks (except those for THF) were present in the product mixture prior to recrystallization. The crystals dissolved readily in CD_3CN, and the solution phase structure appears to be [Tpms^{iPr}ZnCl][LiCl]·2THF. ^{1}H NMR ($CDCl_3$): δ 8.9 (v. br, 3H, 5-pz), 6.3 (br, 3H, 4-pz), 3.75 (m, 8H, THF), 3.3 (m, 3H, Me_2CH), 1.88 (m, 8H, THF), 1.2 (d, 18H, Me_2CH). ^{1}H NMR (CD_3CN): δ 7.54 (br, 3H, 5-pz), 6.38 (s, 3H, 4-pz), 3.64 (m, 8H, THF), 3.24 (m, 3H, Me_2CH), 1.82 (m, 8H, THF), 1.26 (d, 18H, Me_2CH). ^{13}C NMR (CD_3CN): δ 164.3 (3-pz), 137.0 (5-pz), 104.6 (4-pz), 95.9 (C−SO_3), 68.2 (THF), 28.8 (Me_2CH), 26.2 (THF), 23.2 (Me_2CH). IR (CH_2Cl_2): ν 2972 (vs, ν(C−H)), 1533 (m, ν(C═C)), 1054 (vs, ν(S−O)), 639 (vs, ν(C−S)).

Calculation of the Relative Amounts of 8 and $\mathbf{6_{Zn}}$ Resulting from the Reaction between $ZnCl_2$ and 5. In the above procedure in which we prepared crystals of **8**·2THF, prior to recrystallization we took ^{1}H NMR spectra in $CDCl_3$ of the 0.365 g of white solid that resulted after the second filtration. This material was ∼66% by moles or ∼54% by mass **8**, with the remainder being $\mathbf{6}_{Zn}$. Also, the filtrate from the second filtration was analyzed after removing the CH_2Cl_2/hexane solvent. The resulting 0.467 g of a tan solid contained ∼86% by moles or ∼91% by mass $\mathbf{6}_{Zn}$ with the remainder being **8** as observed from the ^{1}H NMR integration.[20] This indicates that the product mixture contained ∼71% $\mathbf{6_{Zn}}$ and ∼29% **8** by mass (or ∼60% and ∼40% by moles, respectively) when $ZnCl_2$ and LiTpms^{iPr} were reacted in a 1.25:1 molar ratio. Additionally, ^{1}H NMR spectra taken prior to workup indicate that $\mathbf{6_{Zn}}$ is the major product in this reaction and that there is no unreacted **5**.

Synthesis of Co(Tpms^{iPr})$_2$ ($\mathbf{6_{Co}}$). Compound $\mathbf{6}_{Co}$ has been prepared from both $CoCl_2$ and $Co(NO_3)_2 \cdot 6H_2O$, but the latter gives purer product. Compound **5** (0.255 g, 0.598 mmol) was mixed with $Co(NO_3)_2 \cdot 6H_2O$ (0.269 g, 0.924 mmol) in 20 mL CH_2Cl_2 for 24 h. The solution was then filtered, and the solvent was removed from the filtrate; the solid was dried under vacuum to give 0.190 g (0.212 mmol) of $\mathbf{6}_{Co}$ in a 70.8% yield. Pink crystals of $\mathbf{6}_{Co}$ for single-crystal X-ray diffraction were grown by slow evaporation of a CH_2Cl_2 solution. ^{1}H NMR (CD_2Cl_2): δ 93.8 (4H, 5-pz Co bound), 64.0

(19) Reger, D. L.; Grattan, C. G.; Brown, K. J.; Little, C. A.; Lamba, J. J. S.; Rheingold, A. L.; Sommer, R. D. *J. Organomet. Chem.* **2000**, *607*, 120−128.

(20) NMR integration values are typically accurate to ±10%, which is a significant source of error in calculating our product ratios.

Scheme 3

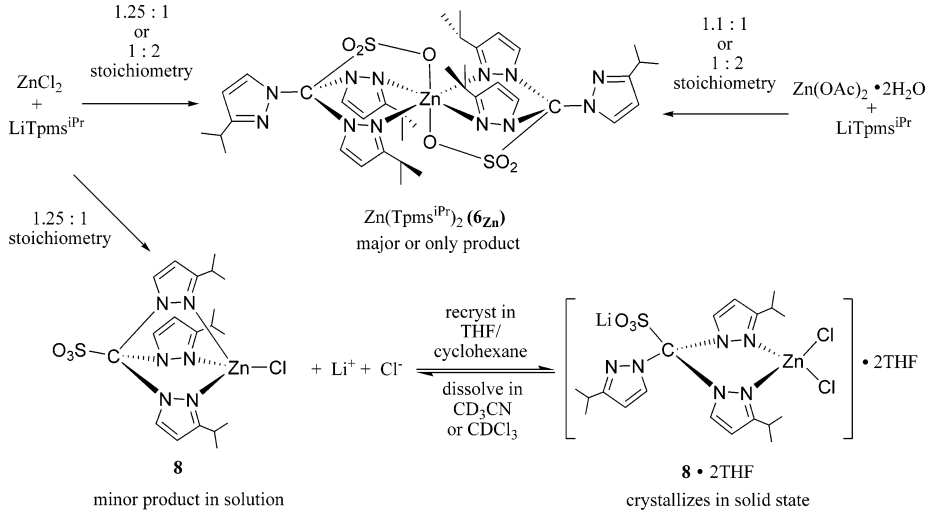

(2H), 43.6 (4H, 4-pz Co bound), 30.5 (2H), 20.7 (2H), 14.8 (12H, *Me*$_2$CH), −37.1 (12H, Me*Me*CH Co bound), −53.6 (12H, *Me*-MeCH Co bound), −153.3 (4H, Me$_2$C*H* Co bound).[21] IR (KBr): ν 3163, 3123 (w, ν(C−H)), 2971 (vs, ν(C−H)), 1541 (m, ν(C═C)), 1044 (vs, ν(S−O)), 653 (vs, ν(C−S)). UV−vis (CH_2Cl_2) (ϵ): 470 (60), 598 nm (35 M^{-1} cm^{-1}). Anal. Calcd: 50.81 C, 6.06 H, 18.73 N. Found: 50.60 C, 5.84 H, 18.37 N.

Synthesis of Ni(Tpms^{iPr})$_2$ (6$_{Ni}$). Compound **5** (0.499 g, 1.17 mmol) was mixed with $NiCl_2$·$6H_2O$ (0.287 g, 1.21 mmol) in 10 mL of CH_2Cl_2, and the mixture was stirred overnight under N_2. The solution was then filtered, and the solvent was removed under vacuum. THF (20 mL) was added, and a light blue solid that would not dissolve was removed by filtration. The light blue solid was dried under vacuum to give 0.101 g (0.113 mmol) of **6**$_{Ni}$ in a 19.3% yield. Light blue crystals of **6**$_{Ni}$ for single-crystal X-ray diffraction were grown by slow evaporation of a CH_2Cl_2 solution. ^{1}H NMR ($CDCl_3$): δ 52 (br, 4H, ^{i}Pr-pz Ni bound), 46 (br, 4H, ^{i}Pr-pz Ni bound), 8.7 (2H, 5-pz), 6.3 (2H, 4-pz), 3.2 (2H, Me$_2$C*H*), 2.1 (br, 12H, *Me*MeCH Ni bound),1.4 (12H, *Me*$_2$CH), −0.5 (v. br., 12H, Me*Me*CH Ni bound), 4H for Me$_2$C*H* Ni bound not observed, probably very broad. IR (KBr): ν 3152 (vw, ν(C−H)), 2965 (vs, ν(C−H)), 1536 (m, ν(C═C)), 1051 (vs, ν(S−O)), 650 (vs, ν(C−S)). UV−vis (CH_2Cl_2) (ϵ): 369 (6.1), 602 nm (2.5 M^{-1} cm^{-1}). Anal. Calcd: 50.82 C, 6.07 H, 18.73 N. Found: 50.57 C, 5.80 H, 18.91 N.

Synthesis of Cu(Tpms^{iPr})$_2$ (6$_{Cu}$). Compound **5** (0.250 g, 0.586 mmol) was mixed with $CuBr_2$ (0.1508 g, 0.675 mmol) in 14 mL of CH_2Cl_2. The reaction was run for 24 h, and the solution was then filtered. The solvent was removed from the filtrate and the solid was dried under vacuum to give 0.0870 g (0.0964 mmol) of **6**$_{Cu}$ in a 32.7% yield. Blue-green crystals of **6**$_{Cu}$ for single-crystal X-ray diffraction were grown by slow evaporation of a CH_2Cl_2 solution. ^{1}H NMR ($CDCl_3$): There were several very broad peaks in the range δ 10−0 and broad, yet distinct, peaks at δ 6.16 (2H, 4-pz), 2.75 (2H, Me$_2$C*H*), 1.04 (12H, *Me*$_2$CH). IR (KBr): ν 2967 (vs, ν(C−H)), 1526 (m, ν(C═C)), 1051 (vs, ν(S−O)), 638 (vs, ν-(C−S)). UV−vis (CH_2Cl_2) (ϵ): 305 (1435), 759 nm (52 M^{-1} cm^{-1}). Anal. Calcd: 50.55 C, 6.03 H, 18.63 N. Found: 50.50 C, 6.26 H, 18.73 N.

Synthesis of Fe(Tpms^{iPr})$_2$ (6$_{Fe}$). Compound **5** (0.322 g, 0.755 mmol) was mixed with $FeCl_2$ (0.150 g, 1.18 mmol) in 20 mL of CH_2Cl_2. The reaction was run for 24 h, and the solution was then filtered. The solvent was removed from the filtrate, and the solid was dried under vacuum to give 0.162 g (0.181 mmol) of **6**$_{Fe}$ in a 47.9% yield. Pale yellow crystals of **6**$_{Fe}$ for single-crystal X-ray diffraction were grown by slow evaporation of a CH_2Cl_2 solution. ^{1}H NMR ($CDCl_3$): δ 47 (br, 4H), 20 (br, 4H), 15 (br, 12H), 2.5 (2H), 1.9 (2H), 0.8 (br, 4H), 0.3 (12H), 0.1 (12H), −1.2 (br, 2H). IR (in CH_2Cl_2): ν 2975 (vs, ν(C−H)), 1527 (m, ν(C═C)), 1041 (vs, ν(S−O)), 653 (vs, ν(C−S)). Anal. Calcd: 50.98 C, 6.09 H, 18.79 N. Found: 51.04 C, 5.96 H, 18.38 N.

Single-Crystal X-ray Diffraction. Structures were solved using direct methods and refined with full-matrix least-squares methods based on F^2 using SHELXTL (G. M. Sheldrick, Madison, WI). The dimeric molecules in LiTpms^{iPr}ZnCl$_2$][THF]$_2$ /[LiTpms^{iPr}ZnCl$_2$]-[THF]·(THF), the tetrameric molecule in NaTpms^{iPr}, and the molecules in Zn(Tpms^{iPr})$_2$, Co(Tpms^{iPr})$_2$, Ni(Tpms^{iPr})$_2$, Cu(Tpms^{iPr})$_2$, and Fe(Tpms^{iPr})$_2$ are located each on inversion centers. All hydrogen atoms were treated as idealized contributions.

Results and Discussion

Synthesis of LiTpms^{iPr} (5). Tris(3-isopropyl-pyrazolyl)-methane (Tpm^{iPr}) of 83% purity was prepared according to Reger's procedure.[19] The mixture of Tpm^{iPr} and its regioisomers was treated with *n*-butyllithium in dry THF at −65 °C, and after deprotonation, SO_3·NMe_3 was added at −45 °C. The reaction produced exclusively 3-substituted LiTpms^{iPr} in a 61% yield (Scheme 2), so presumably only the less hindered Tpm^{iPr} reacted.

Zinc Complexes with the Tpms^{iPr} Ligand. Treating **5** with 1.1 equiv of Zn(OAc)$_2$·$2H_2O$ in CH_2Cl_2 cleanly led to Zn(Tpms^{iPr})$_2$ (**6**$_{Zn}$) in a 74% yield (Scheme 3). **6**$_{Zn}$ was characterized by two types of pyrazole rings in a 1:2 ratio in the ^{1}H NMR. The ^{1}H, ^{13}C, and HMQC NMR spectra (in Supporting Information) reveal three peaks for the methyl groups but only two for the isopropyl C−H groups. This indicates that one isopropyl group on each Zn-bound pyrazole arm has chemically inequivalent methyl groups. X-ray quality crystals were grown by slow diffusion of cyclohexane into THF, and the structure revealed Zn(Tpms^{iPr})$_2$ with an octahedral zinc bound to N,N,O from each ligand (Figure 1, Tables 1 and 2). Apparently, the isopropyl groups have insufficient steric bulk to favor lower coordination numbers.

The addition of NaOH to **6**$_{Zn}$ did not yield the expected Tpms^{iPr}ZnOH but instead produced NaTpms^{iPr} (**7**), as

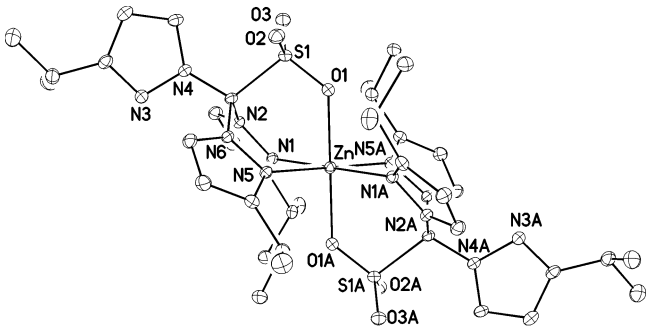

Figure 1. Molecular diagram of $Zn(Tpms^{iPr})_2$. Ellipsoids are shown at 30% probability, and the hydrogen atoms are omitted for clarity.

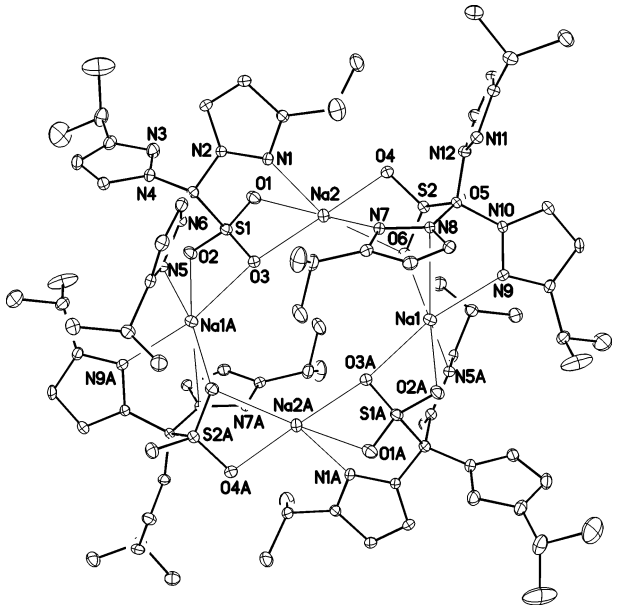

Figure 2. Molecular diagram of $NaTpms^{iPr}$. Ellipsoids are shown at 30% probability, and the hydrogen atoms are omitted for clarity. Selected bond lengths and angles are available as Supporting Information.

characterized by X-ray diffraction (Figure 2, Tables 1 and 3). The crystals have triclinic symmetry in the $P\bar{1}$ space group, and the unit cell contains a tetramer with an inversion center. The two unique sodium environments are both six coordinate distorted octahedral with electrostatic attractions to pyrazole nitrogens and sulfonate oxygens. Other attempts to synthesize $Tpms^{iPr}ZnOH$ or $Tpms^{iPr}ZnOH_2^+$, by reaction of $Zn(Tpms^{iPr})_2$ with $(Bu)_4NOH$ or aqueous AgOTf, show evidence of decomposition in the ^1H NMR. Kitajima et al. noted that treating $Tp^{iPr2}ZnBr$ and $Tp^{iPr2}FeCl$ with NaOH leads to decomposition, but the identity of the products was not discussed.[8a]

The reaction between **5** and $ZnCl_2$ yields two products. Analysis of the ^1H and ^{13}C NMR and IR spectra from the reaction between $ZnCl_2$ and $LiTpms^{iPr}$ in a 1.25:1 molar ratio in methanol indicates that $\mathbf{6}_{Zn}$ is the major product present prior to recrystallization. However, upon recrystallization from THF and cyclohexane, the more polar minor product, $[LiTpms^{iPr}ZnCl_2]\cdot 2THF$ (**8**·2THF), selectively crystallizes out first, as confirmed by single-crystal X-ray diffraction. Two different solvated forms are observed cocrystallized in the crystal phase (Tables 1 and 4). In the solvated form $\mathbf{8}[THF]_2$ (Figure 3), the lithium ions are each coordinated to two THF molecules. In $\mathbf{8}$[THF]·(THF) (Figure 4), a chloride ion displaces one of the THF molecules to become bridging between Zn^{2+} and Li^+. The coordination environment around Li^+ is different in each form, but each Zn^{2+} is in a similar environment with a distorted tetrahedral zinc atom coordinated to N,N,Cl,Cl. The Zn−Cl and Zn−N bond lengths are similar to those seen in known complexes.[13a,17c] Herein, $Tpms^{iPr}$ is acting as a bidentate ligand, in

Table 1. Crystallographic Data for $NaTpms^{iPr}$ (**7**), $[LiTpms^{iPr}ZnCl_2]\cdot 2THF$ (**8**·2THF), and $M(Tpms^{iPr})_2$ ($\mathbf{6}_M$, M = Zn, Co, Ni, Cu, Fe)

	7	**8**•2THF	$\mathbf{6}_{Zn}$	$\mathbf{6}_{Co}\cdot 2CH_2Cl_2$
formula	$C_{76}H_{108}N_{24}Na_4O_{12}S_4$	$C_{108}H_{172}Cl_8Li_4N_{24}O_{20}S_4Zn_4$	$C_{38}H_{54}N_{12}O_6S_2Zn$	$C_{40}H_{58}Cl_4CoN_{12}O_6S_2$
fw	1770.06	2827.78	904.42	1067.83
color/habit	white block	white block	white block	pink block
cryst syst	triclinic	monoclinic	monoclinic	monoclinic
space group	$P\bar{1}$	$P2_1/c$	$P2_1/c$	$P2_1/c$
a (Å)	13.920(5)	16.390(5)	8.805(4)	10.407(3)
b (Å)	14.223(5)	18.811(5)	10.497(4)	21.698(7)
c (Å)	14.960(5)	22.252(6)	23.205(10)	11.368(4)
α (deg)	114.180(4)	90	90	90
β (deg)	91.834(4)	103.588(4)	95.447(6)	108.366(4)
γ (deg)	119.222(4)	90	90	90
V (Å^3)	2255.8(13)	6668(3)	2135.1(15)	2436.3(13)
Z	1	2	2	2
D_{calcd} (g cm^{-3})	1.303	1.408	1.407	1.456
μ (mm^{-1})	0.195	1.004	0.733	0.715
F (000)	936	2960	952	1114
cryst size (mm)	0.22 × 0.18 × 0.12	0.25 × 0.19 × 0.17	0.20 × 0.08 × 0.04	0.30 × 0.20 × 0.15
T (K)	120(2)	120(2)	120(2)	120(2)
λ (Å)	0.71073	0.71073	0.71073	0.71073
θ (deg)	1.73−28.28	1.77−28.31	1.76−28.30	1.88−28.33
no. of measured reflns	12845	37005	23554	26259
no. of observed reflns	8918	14268	4944	5638
GOF	1.010	1.029	1.027	1.014
Final R indices [$I > 2\sigma I$] R_1[a]	5.50	4.40	4.74	6.10
R_2[a]	12.29	9.65	10.82	15.53

	$\mathbf{6}_{Ni}\cdot 2CH_2Cl_2$	$\mathbf{6}_{Cu}$	$\mathbf{6}_{Fe}\cdot 2CH_2Cl_2$
formula	$C_{40}H_{58}Cl_4N_{12}NiO_6S_2$	$C_{38}CuH_{54}N_{12}O_6S_2$	$C_{40}H_{58}Cl_4FeN_{12}O_6S_2$
fw	1067.61	902.59	1064.75
color/habit	light blue block	blue-green block	yellow block
cryst syst	monoclinic	monoclinic	monoclinic
space group	$P2_1/c$	$P2_1/c$	$P2_1/c$
a (Å)	10.388(2)	8.759(3)	10.406(6)
b (Å)	21.628(5)	10.494(3)	21.711(13)
c (Å)	11.372(2)	23.053(7)	11.334(7)
α (deg)	90	90	90
β (deg)	108.252(3)	94.147(4)	108.273(6)
γ (deg)	90	90	90
V (Å^3)	2426.4(9)	2113.5(10)	2431(2)
Z	2	2	2
D_{calcd} (g cm^{-3})	1.461	1.418	1.454
μ (mm^{-1})	0.764	0.676	0.674
F (000)	1116	950	1112
cryst size (mm)	0.40 × 0.35 × 0.20	0.40 × 0.30 × 0.20	0.40 × 0.30 × 0.20
T (K)	120(2)	120(2)	120(2)
λ (Å)	0.71073	0.71073	0.71073
θ (deg)	1.88−28.26	1.77−28.29	2.06−28.34
no. of measured reflns	13403	23193	16275
no. of observed reflns	5311	4948	5459
GOF	1.036	1.042	1.040
Final R indices [$I > 2\sigma I$] R_1[a]	4.25	4.28	7.91
R_2[a]	10.43	12.69	19.18

[a] Quantity minimized = $R(wF^2) = \{\sum[w(F_o^2 - F_c^2)^2]/\sum(wF_o^2)^2\}^{1/2}$; $R(F) = \sum\Delta/\sum(F_o)$, $\Delta = |(F_o - F_c)|$; $w = [\sigma^2(F_o^2) + (aP)^2 + bP]^{-1}$; $P = [2F_c^2 + \max(F_o,0)]/3$.

Table 2. Selected Comparative Bond Distances (Å) and Angles (deg) for M(Tpms^{iPr})$_2$ (**6$_M$**, M = Zn, Co, Ni, Cu, Fe)

6$_{Zn}$		**6**$_{Co}$·2CH$_2$Cl$_2$		**6**$_{Ni}$·2CH$_2$Cl$_2$	
Zn−O(1)	2.0858(18)	Co−O(1)#1	2.0520(19)	Ni−O(1)#1	2.0438(14)
Zn−N(5)	2.135(2)	Co−N(5)	2.144(2)	Ni−N(5)#1	2.0945(19)
Zn−N(1)	2.152(2)	Co−N(1)	2.145(2)	Ni−N(1)	2.0964(17)
N(5)#1−Zn−N(1)	99.41(8)	N(5)#1−Co−N(1)	99.43(8)	N(5)#1−Ni−N(1)	97.76(7)
O(1)−Zn−N(5)#1	92.83(8)	O(1)#1−Co−N(1)	93.60(8)	O(1)−Ni−N(5)#1	92.33(6)
O(1)#1−Zn−N(1)	92.22(8)	O(1)#1−Co−N(5)	91.65(8)	O(1)#1−Ni−N(1)	90.74(6)
O(1)−Zn−N(1)	87.78(8)	O(1)−Co−N(5)	88.35(8)	O(1)−Ni−N(1)	89.26(6)
O(1)−Zn−N(5)	87.17(8)	O(1)−Co−N(1)	86.40(8)	O(1)#1−Ni−N(5)#1	87.67(6)
N(5)−Zn−N(1)	80.59(8)	N(5)−Co−N(1)	80.57(8)	N(5)−Ni−N(1)	82.24(7)

6$_{Cu}$		**6**$_{Fe}$·2CH$_2$Cl$_2$	
Cu−O(1)	2.2446(14)	Fe−O(1)	2.062(3)
Cu−N(5)	2.0190(16)	Fe−N(1)	2.178(3)
Cu−N(1)	2.0326(17)	Fe−N(3)	2.181(3)
N(5)#1−Cu−N(1)	96.67(6)	N(1)#1−Fe−N(3)	100.11(11)
N(5)#1−Cu−O(1)	92.18(6)	O(1)#1−Fe−N(3)	94.16(11)
N(1)#1−Cu−O(1)	91.42(6)	O(1)#1−Fe−N(1)	91.85(11)
N(1)−Cu−O(1)	88.58(6)	O(1)−Fe−N(1)	88.15(11)
N(5)−Cu−O(1)	87.82(6)	O(1)−Fe−N(3)	85.84(11)
N(5)−Cu−N(1)	83.33(6)	N(1)−Fe−N(3)	79.89(11)

Table 3. Selected Bond Distances (Å) and Angles (deg) for NaTpms^{iPr} (**7**)

around Na(1)		around Na(2)	
Na(1)−O(6)	2.262(2)	Na(2)−O(4)	2.294(2)
Na(1)−O(2)#1	2.363(2)	Na(2)−O(3)	2.365(2)
Na(1)−N(9)	2.407(3)	Na(2)−N(1)	2.478(3)
Na(1)−N(5)#1	2.461(2)	Na(2)−N(7)	2.521(2)
Na(1)−O(3)#1	2.473(2)	Na(2)−O(1)	2.667(2)
Na(1)−N(8)	3.058(2)	Na(2)−O(6)	2.689(2)
O(6)−Na(1)−O(2)#1	165.91(9)	O(4)−Na(2)−O(3)	162.43(8)
O(6)−Na(1)−N(9)	83.66(8)	O(4)−Na(2)−N(1)	106.19(8)
O(2)#1−Na(1)−N(9)	107.57(8)	O(3)−Na(2)−N(1)	81.17(8)
O(6)−Na(1)−N(5)#1	104.16(8)	O(4)−Na(2)−N(7)	79.06(8)
O(2)#1−Na(1)−N(5)#1	82.11(7)	O(3)−Na(2)−N(7)	116.66(8)
N(9)−Na(1)−N(5)#1	102.49(9)	N(1)−Na(2)−N(7)	95.52(8)
O(6)−Na(1)−O(3)#1	109.32(8)	O(4)−Na(2)−O(1)	109.53(8)
O(2)#1−Na(1)−O(3)#1	59.71(7)	O(3)−Na(2)−O(1)	56.86(7)
N(9)−Na(1)−O(3)#1	167.01(8)	N(1)−Na(2)−O(1)	71.79(7)
N(5)#1-Na(1)−O(3)#1	74.38(7)	N(7)−Na(2)−O(1)	166.06(8)
O(6)−Na(1)−N(8)	64.60(6)	O(4)−Na(2)−O(6)	56.98(6)
O(2)#1−Na(1)−N(8)	113.01(7)	O(3)−Na(2)−O(6)	119.45(7)
N(9)−Na(1)−N(8)	60.40(7)	N(1)−Na(2)−O(6)	157.52(8)
N(5)#1−Na(1)−N(8)	159.32(8)	N(7)−Na(2)−O(6)	68.09(7)
O(3)#1−Na(1)−N(8)	124.95(7)	O(1)−Na(2)−O(6)	125.69(7)

Table 4. Selected Bond Distances (Å) and Angles (deg) for [LiTpms^{iPr}ZnCl$_2$][THF]·(THF) and [LiTpms^{iPr}ZnCl$_2$][THF]$_2$ (**8**·2THF)

[LiTpms^{iPr}ZnCl$_2$][THF]·(THF)		[LiTpms^{iPr}ZnCl$_2$][THF]$_2$	
Zn(1)−N(1)	2.023(2)	Zn(2)−N(7)	2.025(2)
Zn(1)−N(3)	2.031(2)	Zn(2)−N(9)	2.034(2)
Zn(1)−Cl(2)	2.2241(10)	Zn(2)−Cl(3)	2.2077(8)
Zn(1)−Cl(1)	2.2466(8)	Zn(2)−Cl(4)	2.2324(9)
N(1)−Zn(1)−N(3)	90.96(8)	N(7)−Zn(2)−N(9)	91.54(8)
Cl(2)−Zn(1)−Cl(1)	110.87(3)	N(7)−Zn(2)−Cl(4)	106.63(7)
N(3)−Zn(1)−Cl(1)	110.93(6)	N(9)−Zn(2)−Cl(4)	111.43(6)
N(1)−Zn(1)−Cl(2)	111.87(6)	Cl(3)−Zn(2)−Cl(4)	113.16(3)
N(3)−Zn(1)−Cl(2)	113.73(7)	N(7)−Zn(2)−Cl(3)	115.37(6)
N(1)−Zn(1)−Cl(1)	117.21(6)	N(9)−Zn(2)−Cl(3)	116.55(6)

part, because of the strong electrostatic attraction between Zn−Cl and Li−O$_3$S.

The ^{1}H and ^{13}C NMR spectra of **8**·2THF dissolved in CD$_3$CN or CDCl$_3$ indicate a C_{3v} symmetric complex present in solution, which we propose to have an N,N,N,Cl coordination environment (Scheme 3). Differences between the solid phase and solution structure are presumably because of crystal packing and solvation effects. The mixture that results from a 1.25:1 ratio of ZnCl$_2$ and LiTpms^{iPr} (after workup but prior to recrystallization in THF and cyclohexane) is about 40% **8** and 60% **6**$_{Zn}$ by moles in the ^{1}H NMR in CDCl$_3$. An 8:1

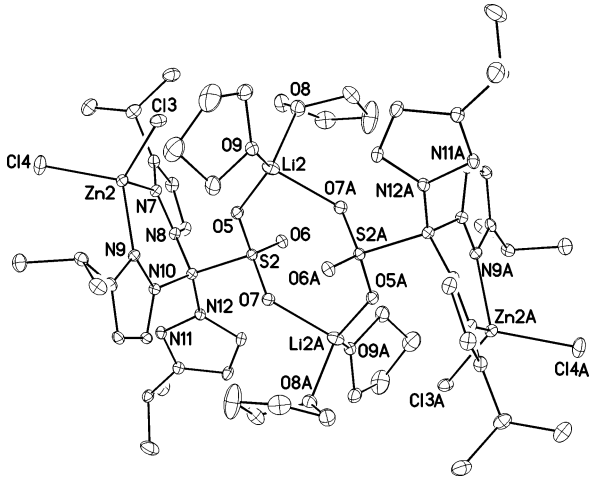

Figure 3. Molecular diagram of [LiTpms^{iPr}ZnCl$_2$][THF]$_2$. Ellipsoids are shown at 30% probability, and the other solvated form and hydrogen atoms are omitted for clarity.

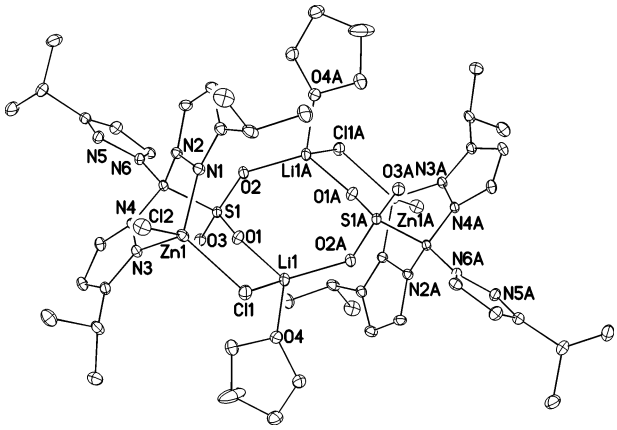

Figure 4. Molecular diagram of [LiTpms^{iPr}ZnCl$_2$][THF]·(THF). Ellipsoids are shown at 30% probability, and the noncoordinated solvent molecule, the other solvated form, and the hydrogen atoms are omitted for clarity.

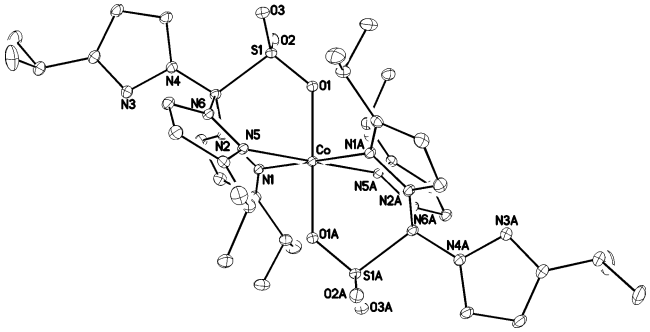

Figure 5. Molecular diagram of Co(Tpms^{iPr})$_2$. Ellipsoids are shown at 30% probability, and the noncoordinated solvent molecules and hydrogen atoms are omitted for clarity.

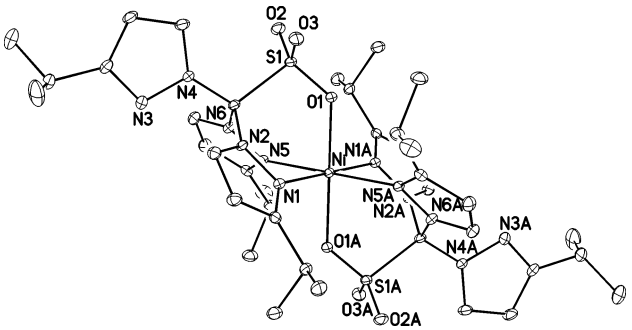

Figure 6. Molecular diagram of Ni(Tpms^{iPr})$_2$. Ellipsoids are shown at 30% probability, and the noncoordinated solvent molecules and hydrogen atoms are omitted for clarity.

molar ratio of $ZnCl_2$ to LiTpms^{iPr} still gives a mixture. However, when $ZnCl_2$ is reacted with LiTpms^{iPr} in a 1:2 molar ratio in methanol, a white solid resulted that is exclusively **6**$_{Zn}$ by ^{1}H NMR.

In summary, $ZnCl_2$ reacts with LiTpms^{iPr} to form a mixture of mostly **6**$_{Zn}$ with **8** as a minor product, whereas $Zn(OAc)_2 \cdot 2H_2O$ reacts with LiTpms^{iPr} to yield exclusively **6**$_{Zn}$. Thus, in both reactions Zn(Tpms^{iPr})$_2$ is the thermodynamically favored product.

Synthesis and Characterization of M(Tpms^{iPr})$_2$ (6$_M$, where M = Co, Ni, Cu, Fe). Although the Tpms^{iPr} ligand binds to zinc through N,N; N,N,N; or N,N,O coordination, the latter is preferred with other metals. Cobalt, nickel, copper, and iron(II) salts gave M(Tpms^{iPr})$_2$ complexes with crystallographically determined similar structures (Scheme 4, Tables 1 and 2, Figures 5−8). The same product resulted

Scheme 4

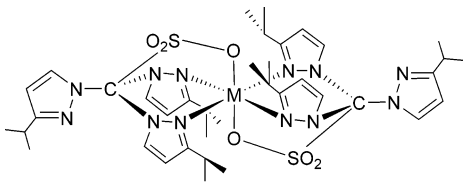

M(Tpms^{iPr})$_2$ (**6$_M$** where M = Cu^{2+}, Ni^{2+}, Co^{2+}, Fe^{2+})

whether we used halide, nitrate, or acetate salts, but the latter two anions typically gave cleaner reactions. The ligand, **5**, is soluble in methanol, water, and other polar solvents because of the sulfonate group. However, in the M(Tpms^{iPr})$_2$ complexes the sulfonate group is buried, and these compounds are insoluble in water.

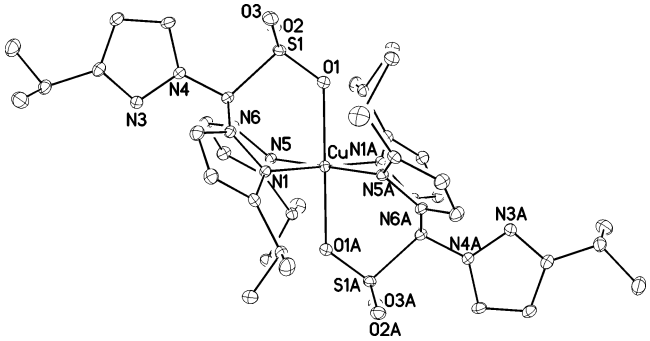

Figure 7. Molecular diagram of Cu(Tpms^{iPr})$_2$. Ellipsoids are shown at 30% probability and the hydrogen atoms are omitted for clarity.

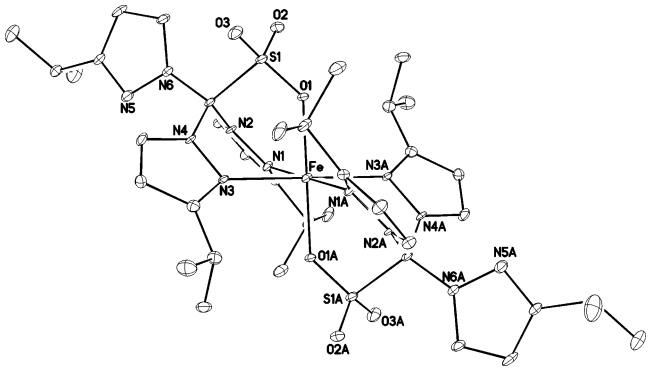

Figure 8. Molecular diagram of Fe(Tpms^{iPr})$_2$. Ellipsoids are shown at 30% probability, and the noncoordinated solvent molecules and hydrogen atoms are omitted for clarity.

Reacting LiTpms^{iPr} with $CoCl_2$ or $Co(NO_3)_2$ in CH_2Cl_2 resulted in a pale pink complex that was recrystallized from CH_2Cl_2 and shown to be Co(Tpms^{iPr})$_2$ by X-ray crystallography (Figure 5). Although solutions of **6**$_{Co}$ slowly decompose if exposed to air for weeks, the complex is stable for weeks in the solid phase and can be kept under N_2 for months with no sign of decomposition. In an attempt to form a cobalt hydroxide complex, 0.3 mL of 1 M NaOH (0.3 mmol) in D_2O was added to an NMR tube containing 10 mg (0.011 mmol) of **6**$_{Co}$ in CD_2Cl_2; no reaction was observed. Thus, **6**$_{Co}$ appears to be more stable toward base than **6**$_{Zn}$. The other sandwich complexes for M = Ni, Cu, and Fe appear to be air stable for short periods of time but were kept under nitrogen as a precaution. Although less hindered four- and five-coordinate Fe(II) complexes are known to easily oxidize,[8a] air stable octahedral iron complexes are not unprecedented.[13a]

Comparison of Bond Lengths and Angles. All of the M(Tpms)$_2$ complexes show a distorted octahedral geometry, but the bond angles around the metal show that the distortion increases in the order Cu < Ni < Zn = Co < Fe, with **6**$_{Fe}$ having two angles are 10° from octahedral. These "sandwich" complexes have inversion centers located at the metal, and the trans angles made by atoms opposite one another in the coordination plane of the metal are all 180°. For zinc, cobalt, nickel, and iron the M−O bond length is shorter than the M−N bond length; the reverse is true for copper. The M−O and M−N bond lengths are similar to those seen in other N,N,O coordination complexes.[13−17]

Table 5. Comparison of UV−vis Spectra for Co(Tpms^{iPr})$_2$, Ni(Tpms^{iPr})$_2$, and Cu(Tpms^{iPr})$_2$ with Known Octahedral Complexes

	donor set	λ_{max} (nm)	λ_{max} (nm)	ref
		$^4T_{1g}(F) \rightarrow {}^4A_{2g}$	$^4T_{1g}(F) \rightarrow {}^4T_{2g}(P)$	
$[Co(1\text{-allylimidazole})_6]^{2+}$	N_6	611	484	23
$[Co(imidazole)_6]^{2+}$	N_6	530	487	24
$[Co(H_2O)_6]^{2+}$	O_6	625	515	24,25
Co[bis(pyrazolyl)methane(phen-2′-olate)]$_2$	N_4O_2	636	464	14a
Co[bis(3,5-dimethylpyrazolyl)methane(phen-2′-olate)]$_2$	N_4O_2	528	434	14a
Co(Tpms^{iPr})$_2$	**N_4O_2**	**598**	**470**	this work
		$^3A_{2g} \rightarrow {}^3T_{1g}(F)$	$^3A_{2g} \rightarrow {}^3T_{1g}(P)$	
$[Ni(1\text{-allylimidazole})_6]^{2+}$	N_6	595	364	23
$[Ni(imidazole)_6]^{2+}$	N_6	575	361	24
$[Ni(H_2O)_6]^{2+}$	O_6	658	395	24,25
Ni[bis(pyrazolyl)methane(phen-2′-olate)]$_2$	N_4O_2	578	362	14b
Ni[bis(3,5-dimethylpyrazolyl)methane(phen-2′-olate)]$_2$	N_4O_2	604	360	14b
Ni(Tpms^{iPr})$_2$	**N_4O_2**	**602**	**369**	this work
		$^2E_g \rightarrow {}^2T_{2g}$		
$[Cu(1\text{-allylimidazole})_6]^{2+}$	N_6	578		23
$[Cu(H_2O)_6]^{2+}$	O_6	794		26
Cu(bis(1-methylimidazol-2-yl)propionate)$_2$	N_4O_2	587		12
Cu(bis(1-methylbenzimidazol-2-yl)propionate)$_2$	N_4O_2	666		12
Cu[bis(3,5-dimethylpyrazolyl)methane(phen-2′-olate)]$_2$	N_4O_2	662		15a
Cu(Tpms^{iPr})$_2$	**N_4O_2**	**759**		this work

Even though homoleptic six coordinate ML_2 complexes are well-known with unhindered tridentate ligands, this result was surprising with isopropyl substituents at the three positions of the pyrazole rings. Kitajima et al. were able to create five-coordinate bimetallic Tp$^{iPr}2_2M_2(\mu\text{-OH})_2$ complexes using isopropyl groups for steric bulk; however, the N,N,N coordination of Tp^{iPr2} brings three isopropyl groups from each ligand toward the metal.[8a] The Tpms^{iPr} ligand appears to favor N,N,O coordination, so similar ligands provide a better basis for comparison. Bis(pyrazolyl)acetate ligands with methyl and *tert*-butyl 3-substituents give octahedral complexes for Fe^{2+},[13b] but the Zn^{2+} complexes of these ligands are primarily tetrahedral (**9**).[13a,c] Similarly, Carrano et al. have used bis(pyrazolyl)methane(phen-2′-olate) derivatives to obtain octahedral Co, Ni, and Cu(II) complexes with methyl 3-substituents,[14,15] but the same ligand gives pseudotetrahedral complexes with Zn^{2+}.[16] However, with isopropyl groups Cu^{2+} complex **10** results.[15a] Although these studies suggest that isopropyl groups on the pyrazole rings are sometimes bulky enough to enforce coordination numbers less than six with N,N,O ligands, clear trends are not evident beyond each individual ligand. Our study of the entire series of late first row transition metals makes it clear that Tpms^{iPr} favors octahedral complexes, even for zinc.

Scheme 5

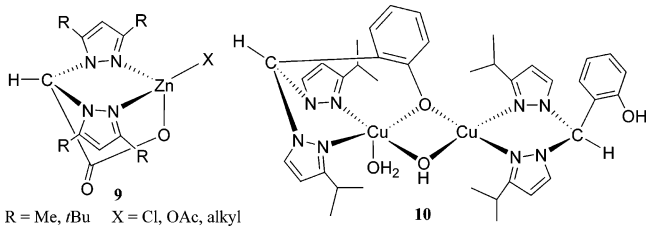

Paramagnetic NMR Spectra and Electronic Configurations. Complex **6**$_{Co}$ is a paramagnetic d^7 complex that has ^{1}H NMR signals between δ 93 and −153 ppm (Supporting Information). The nine observed ^{1}H NMR signals (four for the free pyrazole arms and five for the Co-bound pyrazole arms that have diastereomeric methyl groups) all integrate in the expected ratios and can be assigned by comparison to NMR data of known octahedral Co^{2+} complexes.[21]

A high-spin d^6 configuration for **6**$_{Fe}$ is consistent with its yellow color and the Fe−N bond distances, cf. for high-spin Fe{bis(3,5-dimethylpyrazolyl)acetate}$_2$; Fe−N distances were 2.169 and 2.212 Å. Low-spin iron complexes typically have Fe−N distances 0.2 Å shorter.[13a] The octahedral Fe^{2+} and Ni^{2+} complexes in the literature that have N_4O_2 coordination spheres have similar chemical shifts (δ +56 to −7 ppm)[13a,14b] allowing some peak assignments for **6**$_{Ni}$ and **6**$_{Fe}$.

UV−vis Spectra. 6$_{Co}$ absorbs at λ_{max} = 470 and 598 nm with ϵ = 60 and 35 M^{-1} cm^{-1}, respectively; extinction coefficients below 80 M^{-1} cm^{-1} are characteristic of six-coordinate complexes.[22] Table 5 reports the comparisons of Tpms^{iPr} complexes in this study with those reported for known octahedral complexes with N and O ligands.[23,24,25,26] On the basis of crystal field theory, N_4O_2 donor systems should absorb at wavelengths intermediate between the strong field N_6 and the moderate field O_6 donor sets. This appears to be the case for **6**$_{Ni}$ which absorbs at 602 nm as compared to 595 nm for $[Ni(1\text{-allylimidazole})_6](NO_3)_2$ and 658 nm for $[Ni(H_2O)_6]^{2+}$. Similarly, λ_{max} for **6**$_{Cu}$ is 759 nm which lies between 578 (N_6) and 794 nm (O_6). The λ_{max} values observed for **6**$_{Co}$ are lower than those reported for $[Co(1\text{-allylimidazole})_6]^{2+}$ by 13−14 nm, but they are still close enough to be considered indicative of octahedral geometry. This simplistic

(21) Rheingold, A. L.; Yap, G. P. A.; Zakharov, L. N.; Trofimenko, S. *Eur. J. Inorg. Chem.* **2002**, 2335−2343. For paramagnetic Co^{2+} complexes, chemical shift is related to distance from the metal: (b) La Mar, G. N.; Van Hecke, G. R. *J. Am. Chem. Soc.* **1970**, *92*, 3021−3028.
(22) Rosenberg, R. C.; Root, C. A.; Wang, R.; Cerdonio, M.; Gray, H. B. *Proc. Natl. Acad. Sci. U.S.A.* **1972**, *70*, 161−163.
(23) Kurdziel, K.; Głowiak, T. *Polyhedron* **2000**, *19*, 2183−2188.
(24) Eilbeck, W. J.; Holmes, F.; Underhill, A. E.; *J. Chem. Soc., Sect. A* **1967**, 757.
(25) Underhill, A. E.; Billing, D. E. *Nature* **1966**, *210*, 834.
(26) Lever, A. B. P. *Inorganic Electronic Spectroscopy*, 2nd ed.; Elsevier: New York, 1984.

analysis overlooks changes in the d orbital energy levels from Jahn−Teller distortion, but the M−O and M−N bond lengths are similar enough to justify this approach for Co and Ni. Additionally, for $\mathbf{6}_{Co}$ and $\mathbf{6}_{Ni}$, the λ_{max} values are similar to those of known octahedral complexes with N_4O_2 donor sets. For $\mathbf{6}_{Cu}$, the absorbance is ∼100 nm greater than that for known N_4O_2 complexes, but our Cu−O distances are also 0.11 Å shorter than those reported for Cu(bis(1-methylbenzimidazol-2-yl)propionate)$_2$, and electronic differences are possible because of either the unique donor properties of the sulfonate group or the extent of the Jahn−Teller distortion.

Conclusions

The Tpms^{iPr} ligand forms octahedral M(Tpms^{iPr})$_2$ complexes from various divalent metal salts, solvents, and stoichiometric ratios, despite the crowded appearance of the isopropyl groups in the crystal structures. These mononuclear six coordinate complexes are very surprising since in other ligands 3-isopropylpyrazole rings led to the formation of bridged bi- or trimetallic complexes,[14a,b] some of which had lower coordination numbers.[8a,15a] The present study confirms previous work that, despite free sulfonate being generally regarded as a noncoordinating anion, N,N,O binding is usually favored for Tpms scorpionates,[17,18] which places only two isopropyl groups from each ligand near the metal. This does not explain how other N,N,O complexes containing 3-isopropylpyrazole rings, such as **10**, can be four or five coordinate. In this case, the difference is likely to be the result of either the propensity of phenolate to act as a bridge or the steric differences between the ligands. It is clear that steric effects must be considered a function of the entire ligand backbone, and isopropyl groups are not always sufficient to favor lower coordination numbers, even for typically tetrahedral metals such as zinc.

In conclusion, Tpms^{iPr} is significantly less bulky than Tpms^{tBu},[17] and we see predominantly octahedral sandwich complexes. These complexes are good structural models for facial N,N,O coordination in 2-His-1-carboxylate enzymes. M(Tpms^{iPr})$_2$ complexes provide a spectroscopic signature for octahedral metals in similar environments and represent the first homologous series of Zn, Cu, Ni, Co, and Fe complexes from a ligand with N,N,O donor atoms.

Acknowledgment. The authors thank the ACS Petroleum Research Fund (Grant 435120) and the Henson school for financial support, Dr. J. R. Norton, Dr. D. F. Rieck, Dr. C. H. Yoder, and Dr. M. O. Mitchell for helpful discussions, and P. Clements and C. R. Ekeocha for assistance with experiments.

Supporting Information Available: Further experimental details, ^{1}H, ^{13}C, and HMQC NMR and IR spectra, and crystallographic data. This material is available free of charge via the Internet at http://pubs.acs.org. Crystal structures are available from the Cambridge Crystallographic Data Centre under depositary numbers CCDC 277094−277096, 283435−283439.

IC051579A